

GENERAL ARTICLE

Biallelic variants in FBXL3 cause intellectual disability, delayed motor development and short stature

Muhammad Ansar^{1,†}, Sohail Aziz Paracha^{2,†}, Alessandro Serretti³, Muhammad T. Sarwar², Jamshed Khan², Emmanuelle Ranza^{1,4}, Emilie Falconnet¹, Justyna Iwaszkiewicz⁵, Sayyed Fahim Shah⁶, Azhar Ali Qaisar⁷, Federico A. Santoni^{1,8}, Vincent Zoete^{5,9}, Andre Megarbane¹⁰, Jawad Ahmed², Roberto Colombo^{11,12}, Periklis Makrythanasis^{1,13} and Stylianos E. Antonarakis^{1,4,14,*}

¹Department of Genetic Medicine and Development, University of Geneva, 1211, Geneva, Switzerland,

²Institute of Basic Medical Sciences, Khyber Medical University, 25100, Peshawar, Pakistan, ³Department of

Biomedical and Neuromotor Sciences, University of Bologna, 40126, Bologna, Italy, ⁴Service of Genetic

Medicine, University Hospitals of Geneva, 1205, Geneva, Switzerland, ⁵Swiss Institute of Bioinformatics,

Molecular Modeling Group, Batiment Genopode, Unil Sorge, 1015, Lausanne, Switzerland, ⁶Department of

Medicine, KMU Institute of Medical Sciences, 26000, Kohat, Pakistan, ⁷Radiology Department, Lady Reading

Hospital, 25100, Peshawar, Pakistan, ⁸Department of Endocrinology Diabetes and Metabolism, University

Hospital of Lausanne, 1011, Lausanne, Switzerland, ⁹Department of Fundamental Oncology, Lausanne

University, Ludwig Institute for Cancer Research, Route de la Corniche 9A, 1066 Epalinges, Switzerland,

¹⁰Institut Jerome Lejeune, 75015, Paris, France, ¹¹Institute of Clinical Biochemistry, Faculty of Medicine,

Catholic University IRCCS Policlinico Gemelli, 00136, Rome, Italy, ¹²Center for the Study of Rare Hereditary

Diseases, Niguarda Ca' Granda Metropolitan Hospital, 20162, Milan, Italy, ¹³Biomedical Research Foundation of

the Academy of Athens, 115 27, Athens, Greece and ¹⁴iGE3 Institute of Genetics and Genomics of Geneva, 1211,

Geneva, Switzerland

*To whom correspondence should be addressed at: University of Geneva Medical School, Department of Genetic Medicine and Development 1 Rue Michel Servet, 1211 Geneva, Switzerland. Tel: +41 22 37 95708; Fax: +41-22-379-5706; Email: stylianos.antonarakis@unige.ch

Abstract

FBXL3 (F-Box and Leucine Rich Repeat Protein 3) encodes a protein that contains an F-box and several tandem leucine-rich repeats (LRR) domains. FBXL3 is part of the SCF (Skp1-Cullin-F box protein) ubiquitin ligase complex that binds and leads to phosphorylation-dependent degradation of the central clock protein cryptochromes (CRY1 and CRY2) by the proteasome and its absence causes circadian phenotypes in mice and behavioral problems. No FBXL3-related phenotypes have been described in humans. By a combination of exome sequencing and homozygosity mapping, we analyzed two consanguineous families with intellectual disability and identified homozygous loss-of-function (LoF) variants in FBXL3. In the first family, from Pakistan, an FBXL3 frameshift variant [NM_012158.2:c.885delT:p.(Leu295Phefs*25)] was the only

[†]These authors contributed equally to this work.

Received: September 18, 2018. Revised: November 13, 2018. Accepted: November 14, 2018

© The Author(s) 2018. Published by Oxford University Press. All rights reserved.

For Permissions, please email: journals.permissions@oup.com

segregating variant in five affected individuals in two family loops (LOD score: 3.12). In the second family, from Lebanon, we identified a nonsense variant [NM_012158.2:c.445C>T:p.(Arg149*)]. In a third patient from Italy, a likely deleterious non-synonymous variant [NM_012158.2:c.1072T>C:p.(Cys358Arg)] was identified in homozygosity. Protein 3D modeling predicted that the Cys358Arg change influences the binding with CRY2 by destabilizing the structure of the FBXL3, suggesting that this variant is also likely to be LoF. The eight affected individuals from the three families presented with a similar phenotype that included intellectual disability, developmental delay, short stature and mild facial dysmorphism, mainly large nose with a bulbous tip. The phenotypic similarity and the segregation analysis suggest that FBXL3 biallelic, LoF variants link this gene with syndromic autosomal recessive developmental delay/intellectual disability.

Introduction

Intellectual disability (ID), a common neurodevelopmental disorder, is characterized by significant deficiency of cognitive functions and impairment of at least two adaptive skills before the age of 18 years (1,2). It is one of the major public health problems because of its clinical and etiological heterogeneity and the lack of diagnostic and therapeutic options. It seriously impacts on the quality of life of affected individuals and their families and poses a substantial socio-economic burden to the health care system (3,4). The prevalence of ID is 1–3% in the population worldwide; however, its prevalence is almost twice in the developing world (5,6). To date ~700 protein-coding genes have been implicated in ID (7) and approximately half of them have an autosomal recessive pattern of inheritance (8–11).

Autosomal recessive disorders are common in populations where consanguineous marriages are frequent and consanguinity is considered as one of the major contributing factors of child morbidity and mortality (12–18). Studying consanguineous families with more than one affected offspring has proven to be an effective strategy to discover causative pathogenic variants in novel recessive genes and improve genetic diagnosis (15,19).

A combined approach of exome sequencing of one proband per family and genotyping all the available family members to perform homozygosity mapping is a powerful strategy to identify the molecular cause of the phenotype in consanguineous families (20–26). We recruited two unrelated consanguineous families with ID, developmental delay and short stature phenotypes and found two homozygous loss-of-function (LoF) variants in FBXL3 (F-Box and Leucine Rich Repeat Protein 3; OMIM#605653): a nonsense codon in the first (NM_012158.2:c.445C>T:p.(Arg149*) and a frameshift deletion in the second [NM_012158.2:c.885delT:p.(Leu295Tyrfs*25)]. The variants segregated with the disease phenotype. A third homozygous, non-synonymous likely LoF variant [NM_012158.2:c.1072T>C:p.(Cys358Arg)] was identified in a patient originating from Italy with a similar phenotype.

Results

Clinical evaluation

The highly consanguineous family F145 included five affected individuals (IV:5, IV:6, IV:7, IV:8 and V:2) in two generations (Figs 1A and D). All affected subjects were clinically evaluated and presented with mild to severe ID, developmental delay, short stature (<1st centile) and mild facial dysmorphism such as a broad nasal bridge and relatively large nose with bulbous tip (Fig. 1D). All developmental milestones, including speech, fine motor, gross motor and social behavior, were delayed. Secondary sexual characteristics were only partially developed in all affected subjects.

In the second consanguineous family F002 (Fig. 1B), there were two affected sisters (IV:1 and IV:2). Pregnancies were unremarkable. Birth parameters are unavailable, but they were reported by the mother to be within normal limits. The third sister (IV:3) died of leukemia at the age of 15 years without evidence of developmental delay or ID. The age of the affected females IV:1 and IV:2 at the time of clinical evaluation was 35 and 34 years, respectively. Both presented with ID, developmental delay, dysarthric speech, short stature (<1 centile), joint hyperlaxity and dislocation and mild facial dysmorphism including a broad nasal bridge and a relatively long nose with bulbous tip having a slight median groove, microretrognathism and high arched palate. Radiographic examinations revealed the presence of widened mandibular angles, hypoplastic clavicles, short distal ends of ulnae, short fourth metacarpals and dislocation of hip, elbows and thumb joints. Detailed clinical evaluations of the family F002 are reported previously (27).

In family F145, X-rays of pelvis anteroposterior (AP), chest/thorax posteroanterior (PA) and hands/wrists AP and lateral view regions taken in all the five affected individuals (IV:5, IV:6, IV:7, IV:8 and V:2) and brain MRI scans performed in one affected (IV:6) did not reveal any abnormality. All the biochemical and radiological tests were normal. No skeletal abnormalities (joint laxity or dislocations) were observed.

The proband of family M213 (Fig. 1C) is a 23-year-old male (VI:2) born to distally consanguineous parents after an uncomplicated pregnancy. His birth parameters were the following: weight, 2800 g ($Z = -0.8$); length, 46 cm ($Z = -1.4$); and head circumference, 31 cm ($Z = -2$). In the neonatal period, he had weight loss due to feeding difficulties and was tube-fed for 2 months. There was no history of seizures. Developmental delay first became evident at the age of 5 months. All milestones of motor development were delayed: he sat with support at 12 months, rolled over at 12 months, crawled at 18 months and walked at 30 months. Speaking emerged at the age of 2 years and 6 months. At the beginning of school age, he only spoke up to 5-word sentences, used supportive sign language and had dysarthria. Upper respiratory tract infections in childhood were frequently present. Psychological examination at the age of 20 years showed moderate ID. Full scale, verbal and performance IQ (Wechsler Adult Intelligence Scale; WAIS-R) (28) were 48, 53 and 43, respectively. Mini-Mental State Examination (Folstein Test (29)) and Rey–Osterrieth Complex Figure Test, immediate recall and delayed recall (30) resulted in the following scores (cut-off score): 20.5 (23.8), 22 (28.9) and 4.5 (9.5), respectively. Working memory was assessed by the Frontal Assessment Battery (31) and the Raven's Colored Progressive Matrices (32,33) for which the following scores were recorded: 8 (16.5) and 14.7 (19), respectively. Last, visuospatial processing was evaluated by the Rey's Complex Figure Copy Test (34) and the Benton's Judgment of Line Orientation Test (35) the resulted in the following scores: 14 (34) and 13 (20), respectively. Sleep disturbances

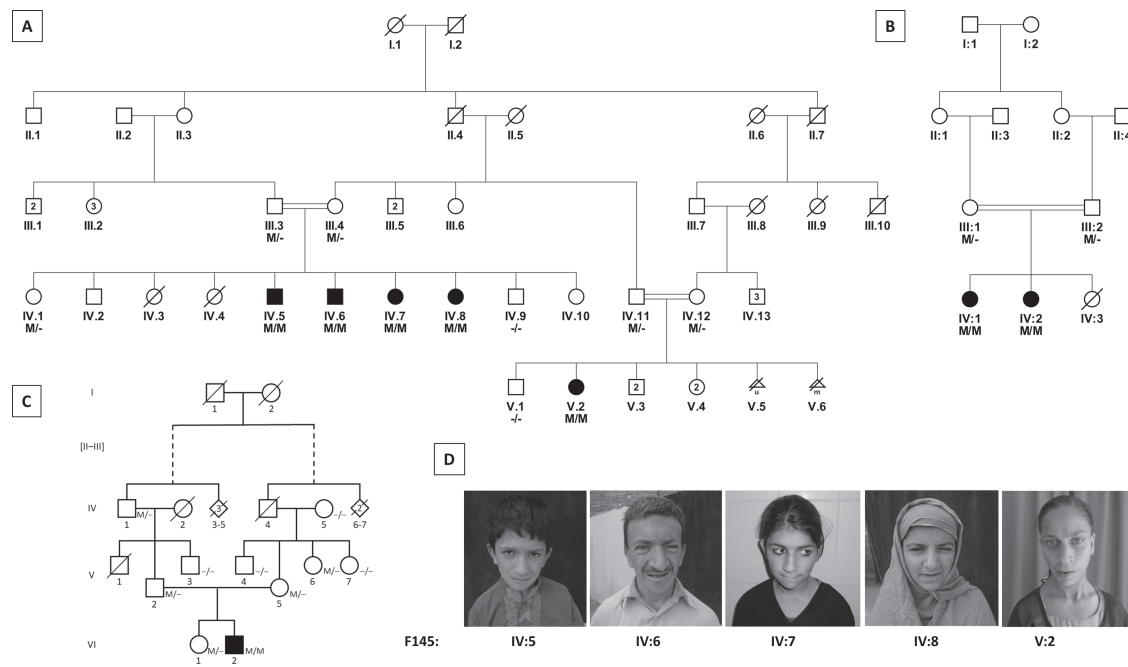


Figure 1. Family pedigrees and segregation of variants: pedigrees of the families with *FBXL3* (NM_012158.2) variants. (A) Family F145 with homozygosity c.884delT:p.(Leu295Tyrfs*25). (B) Family F002 with homozygosity for c.445C>T:p.(Arg149*) in *FBXL3*. (C) Family M039 with homozygosity c.1072T>C; p.Cys358Arg. (D) Photographs of five affected individuals of family F145; photographs and clinical features of the two affected individuals of family F002 have already been reported in (27). Permission to publish the photograph of the affected individual of family M213 was not granted. However, the clinical facial features of that individual are similar to the affected individuals of families F145 and F002. M/M, subjects homozygous for the *FBXL3* likely pathogenic variant; M/–, mutation carrier; –/–: subjects with wild-type *FBXL3* alleles.

were reported by parents since the proband was a child, but neither polysomnography nor electroencephalograph recording was available to the investigators at the time of the present study. Numerous night awake episodes (>10 min) were present since the first decade of life and their number and duration increased in the following decade, especially during some periods of the years, reducing considerably the average number of sleeping hours during the night (≤ 5). On the day side, the patient, if not prevented in doing this by his parents or unfavorable circumstances, may sleep for up to 2–3 hours during the period of natural light. As a treatment of his irregular sleep–wake rhythm, the boy received melatonin as a dietary supplement during adolescence (≤ 10 mg/daily) and up to 19 years of age, and low doses of sedative-hypnotics (benzodiazepines) during the following years.

Detailed clinical phenotypes of all affected individuals are listed in Table 1.

Genetic analysis

In families F145 and F002, 97% of the Refseq protein coding exons (NM_012158.2) were covered at least 10 \times . Exome sequencing of individual IV:8 of family F145 yielded 23 663 high quality exonic and splice junction variants, while in case of family F002, exome sequencing was performed in individual IV:2 and yielded such 22 022 variants. Initial analysis of the exome data excluded any pathogenic, likely pathogenic or variants of unknown significance in genes known to cause ID. Genotyping of individuals III:3, III:4, IV:1, IV:6, IV:7 and IV:8 in family F145 and III:1, III:2, IV:1 and IV:2 in family F002 was then performed as described. Run of homozygosity (ROH) was calculated in each individual, and the variants present in the ROH segregating with the disease phe-

notype in each family were isolated and analyzed by the CATCH (36) program. Segregation of the variants is further verified in all available individuals of each family through Sanger sequencing.

The analysis of family F145 revealed only one candidate homozygous frameshift variant NM_012158.2:c.884delT:p.(Leu295Tyrfs*25) in *FBXL3*. In family F002, three homozygous variants NM_012158.2:c.445C>T:p.(Arg149*) in *FBXL3*, NM_006238.4:c.29A>C:p.(Glu10Ala) in *PPARD* (OMIM#600409) and NM_005358.5:c.1532A>G:p.(Glu511Gly) in *LMO7* (OMIM* 64362) segregated with the disease phenotype. Out of three segregating variants, we focused on *FBXL3* for two reasons, (1) the variant p.(Arg149*) is LoF and (2) phenotypes of both affected individuals, especially facial dysmorphism, were very similar to patients of family F145, where we have found the other LoF variant in *FBXL3*. We have hypothesized that the skeletal abnormalities (joint laxity or dislocations) in affected individuals of family F002 could be caused by one of other two segregating variants, *PPARD*: p.(Glu10Ala) or *LMO7*: p.(Glu511Gly). *PPARD* has been reported to be involved in the development of cartilage (37), so it could be a good candidate for skeletal phenotypes.

In family M213, exome sequencing of the proband (VI:2) and his parents (V:2 and V:5) yielded >22000 reliable exonic variants. By performing trio-analysis, the only candidate variant that remained after the filtering steps for frequency in the general population, predicted pathogenicity and segregation studies by Sanger sequencing was *FBXL3* (chr13:77581495A>G; c.1072T>C; p.Cys358Arg). The *FBXL3* c.1072T>C variant, identified in the homozygous state in the proband, is novel, was inherited from his heterozygous parents (V:2 and V:5) and was also identified in heterozygosity in one maternal aunt (V:6) and the paternal grandfather (IV:1), all of which are unaffected. This missense

Table 1. Anthropometric and clinical features of affected individuals

	Family F145				Family F002			Family M213
	IV:5	IV:6	IV:7	IV:8	V:2	IV:1	IV:2	VI:2
	Male	Male	Female	Female	Female	Female	Female	Male
Age at last evaluation (years)	8.6	27	12	15	22.5	35	34	23
Height (cm)	112	153	128	137	161	NA	NA	151
Stature	Short	Short	Short	Short	Short	Short	Short	Short
Head circumference (cm)	53 (68th percentile, Z = + 0.5)	58 (98th percentile, Z = + 2)	51 (4th percentile, Z = - 1.7)	55 (75th percentile, Z = + 0.7)	51 (<1st percentile, Z = - 3.1)	NA	NA	53 (11th percentile, Z = - 1.2)
ID	Mild	Moderate to severe	Mild to moderate	Severe	Moderate	Severe	Severe	Moderate
Developmental delay	Yes	Yes	Yes	Yes	Yes	Yes	Yes	Yes
Speech	Delayed	Slurred speech	Delayed	Slurred speech	Dysarthria	Dysarthria	Dysarthria	Dysarthria
Motor milestones	Delayed	Delayed	Delayed	Delayed	Delayed	Delayed	Delayed	Delayed
Behavioral problems	No	No	Aggressive	Odd and shy	No	No	No	Odd, shy and under-responsive to stimuli
Fascial dysmorphism	Large bulbous nose, microretrognathism	Large bulbous nose, microretrognathism	Large bulbous nose	Large bulbous nose	Large bulbous nose, microretrognathism	Large bulbous nose, microretrognathism	Large bulbous nose, microretrognathism	Large bulbous nose
Eye problems	No	Strabismus	No	Strabismus	No	Ptosis	No	Ptosis
Circadian rhythm	No	No	No	No	No	No	No	Yes
Other symptoms						Hyperlaxity and dislocation of hip, elbows and thumb joints	Hyperlaxity and dislocation of hip, elbows and thumb joints	

Clinical evaluations of affected individuals: Detailed clinical features of all affected individuals from three unrelated families F145, F002 and M213 are described in the table.

FBXL3 mutation was transmitted to the family by one of its progenitors (I:1 or I:2) who settled in the 19th century in the small village of origin of the family.

Protein modeling

FBXL3 is an arch-shaped protein with solenoid fold that is interacting with CRY1 and CRY2 cryptochrome proteins. The structure of human FBXL3 was crystalized with a murine CRY2 protein that shares 94.27% sequence identity with a human CRY2 homologue (38). In this complex, the N-terminal F-box domain of FBXL3 interacts with the adaptor protein SKP1, whereas the C-terminal leucine-rich repeat (LRR) domain interacts with CRY2 protein. The LRR domain consists of 12 LRRs adapting together a form of a semi-circular arch. Each LRR comprises one alpha helix followed by a beta strand. The alpha helices are forming the outside surface of the arch and the beta strands, arranged in a parallel beta-sheet, are forming the inside surface of the arch. The concave surface of FBXL3 wraps around the alpha-helical domain of CRY2. In the complex only the C-terminal part of LRR domain semicircle (LRR7–LRR12) forms the tight

hydrophobic contacts with CRY2, while the N-terminal part of LRR domain interacts with CRY2 only via few hydrogen bonds. The importance of C-terminal part of LRR domain for the interaction with CRY2 was confirmed by mutagenesis studies (38).

Taking into account the importance of the C-terminal part of LRR domain for the CRY2 protein interaction the deletion with frameshift on residue Leu295 that affects the structure of the LRR7 repeat and the nonsense mutation Arg149 that affects the LRR4 repeat must result in structures of FBXL3 that are too short to efficiently interact with CRY2.

The third investigated mutation, Cys358Arg affects the same codon position as described already, the murine *Fbxl3* variant Cys358Ser, known as ‘after hours’ mutation, that perturbs the mouse circadian rhythm by prolonging the cycle to 27 h (39,40).

The Cys358 residue does not interact directly with the CRY2 as its side chain points towards inside of the structure (Fig. 2B) and it is interacting with hydrophobic residues Val237, Leu334, Ile354 and Leu361 that are forming the hydrophobic core of LRR10. Additionally, Cys358 forms the hydrogen bond interactions with the backbone of LRR9 repeat (Fig. 2B). The mutation

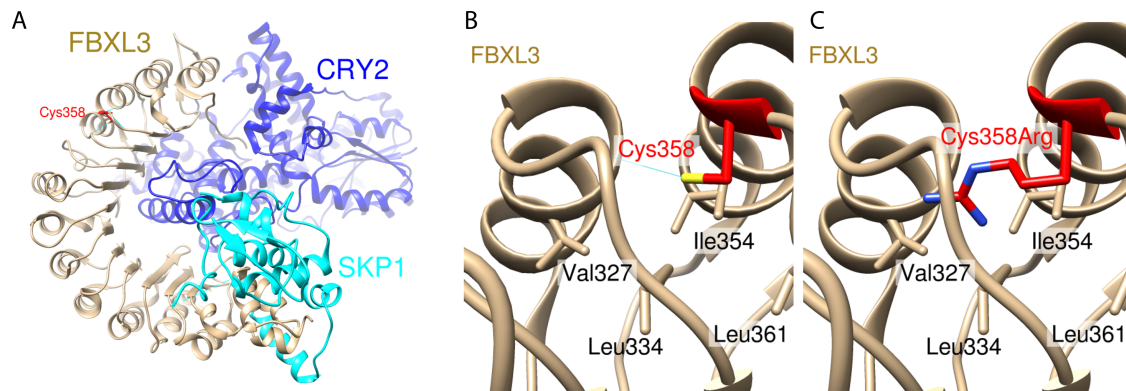


Figure 2. Protein molecular modeling of the FBXL3 missense variant Cys358Arg: FBXL3 is in beige, CRY2 in dark blue, SKP1 in cyan. Cys358 and Cys358Arg residues are in red. (A) A general overview of FBXL3 with its LRRs, showing that Cys358 is positioned on the 10th LRR motif forming a solenoid around CRY2. (B) Zoom in of the Cys358 that is pointing towards inside of the structure and the Cys358 side chain is interacting with hydrophobic residues Leu334, Ile354, Leu361 and Val327. (C) Zoom in of the mutant Cys358Arg showing that Arg358 would destabilize the fold, as its side chain is big, long and charged, and therefore it might influence the CRY2 binding through partial destabilization of the FBXL3 structure.

to a much longer and charged residue of arginine most likely perturbs the LRR10 structure. The longer arginine side chain most likely produces clashes with surrounding residues and its highly polar guanidinium group interacts unfavorably with the hydrophobic environment of LRR10 core (Fig. 2C).

As we estimated using the FoldX software (41) the Cys358Arg variant accounts for 9.7 kcal/mol loss of stability of FBXL3 protein. This mutation destabilizes therefore the structure of LRR domain and leads most probably to the impairment of FBXL3/CRY2 interactions.

Discussion

We report seven individuals from two consanguineous families with two different LoF variants p.(Leu295Tyrfs*25) and p.(Arg149*) in FBXL3 and a single patient from another family with a missense variant p.(Cys358Arg). All patients presented similar clinical features of ID, short stature and mild facial dysmorphism. The single patient with the nonsynonymous variant p.(Cys358Arg) also showed disturbed sleep-wake cycle.

FBXL3 contains an F-box domain that includes a 40 amino acid motif for protein-protein interactions and 12 tandem LRRs labeled Fbxl3-LRR domains that mediate substrate recognition (42). FBXL3 is a part of the SKP1-CUL1-F-box-protein (SCF) complex that largely functions within the cell nucleus and facilitates ubiquitination by degrading cryptochrome proteins (CRY1 and CRY2) (43–45). FBXL3 contributes in molecular events of circadian rhythm of mammals by affecting negative feedback loop through binding to cryptochrome proteins to expedite their SCF complex-mediated polyubiquitination and their subsequent degradation by the proteasome (43,46,47). Substrate recognition site of SCF(FBXL3) E3 ubiquitin ligase complex is responsible for circadian rhythm function and is important to maintain speed and robustness of the oscillation of circadian clock (43–45).

In an *in vitro* study, the transfection of p.(Cys358Ser) and p.(Cys358Ala) mutants were shown to interfere and abolish the interaction of FBXL3 with CRY1 and CRY2 (48). In mice *Fbxl3* has a fundamental role to regulate the CRY protein (49). *Fbxl3* mutant p.(Cys358Ser) mouse models have been associated with disturbances of the circadian rhythm and behavioral problems such as reduced anxiety, depression-like behavior and memory defects in some tests (39,40). In a study conducted under the IMPC consortium, the *Fbxl3* knockout mice had significantly

disturbed center average speed compared with controls (<https://www.mousephenotype.org>). The mouse p.(Cys358Ser) allele resembles closely that of our reported patient of family M213 with the homozygosity p.(Cys358Arg) in which we have observed a disturbed sleep pattern. We hypothesize that the missense variant at position Cys358 results in the circadian phenotype in human and mice because of the defective interaction with CRY1 and CRY2 (48). Cognitive deficits observed in *Fbxl3* p.(Cys358Ser) mutant mice were only found in some tests (39,40). *Fbxl3* knockout mice showed disturbed circadian clock (50); however, we did not observe a severe disturbance of circadian rhythm in the patients with homozygous nonsense FBXL3 variants [p.(Leu295Tyrfs*25) and p.(Arg149*)]. This could be due to differences between human and mouse, inability to detect mild differences in circadian rhythm in patients or the existence of an alternative molecular pathway that compensates the absence of FBXL3 function in humans.

Irregular sleep-wake rhythms have been reported in patients with developmental delay and ID (51,52). Other F-box proteins such as FBXO31 and FBXO28 are already been implicated in ID and developmental delay phenotypes (53,54), with some specific clinical features of a broad nasal bridge, bulbous nasal tip (53), short stature and sleep difficulties (54) similar to what we have observed in the affected individuals described here with FBXL3 homozygous null variants.

In summary, we conclude that homozygous FBXL3 LoF variants likely cause autosomal recessive ID, short stature, developmental delay and facial dysmorphism in humans, and that the Cys358Arg FBXL3 variant likely adds the circadian phenotype because of abnormal interaction with CRY1 and CRY2. Further functional studies are necessary to explore the molecular pathophysiology of this gene-phenotype link.

Materials and Methods

Study participants

The three investigated families and their pedigrees are reported in Figure 1. The first family (F145) was recruited at the Institute of Basic Medical Sciences, Khyber Medical University, Peshawar, Pakistan and the second (F002) was identified at the Unité de Génétique Médicale, Faculté de Médecine, Université St Joseph, Beirut, Lebanon. Both families F145 and F002 were studied at the Department of Genetic Medicine and Development, University of

Geneva, Geneva, Switzerland. The third patient's family (M039) originated from a small Italian village. A genealogic investigation by interviews and inspection of civil and parish registers revealed that the proband's parents share a common ancestor dating back to the 19th century. The study was approved by the Bioethics Committee of the University Hospitals of Geneva (Protocol number: CER 11-036). Written informed consent was obtained from the members of the three families and the study was performed according to the Helsinki declaration.

Exome sequencing, genotyping and data analysis

Exome capture was performed using SureSelect Human All Exon v4 kit (Agilent Technologies, Santa Clara, CA, USA) for families F002 and M213, and SureSelect Human All Exon v6 reagent (Agilent Technologies) for F145. The captured libraries were sequenced on the Illumina HiSeq 2500 (F002 and M039) and HiSeq 4000 (F145) platforms (Illumina Inc., San Diego, CA, USA). The bioinformatics analysis of exome data was carried out using in-house customized pipelines based on published algorithms that include Burrows–Wheeler aligner tool BWA (55), SAMtools (55), PICARD (<http://broadinstitute.github.io/picard/>) and GATK (56). The human reference genome (GRCh37/hg19) (57) was used for mapping. Initial screening for known or likely pathogenic variants was performed in genes already known to cause developmental delay and ID. A total of 720 K-SNP microarray hybridization (HumanOmniExpress Bead Chip by Illumina Inc.®) was performed to genotype all members of families F002 and F145 (average SNP density 4 kb). PLINK (58) was used to perform homozygosity mapping. ROHs were described as genomic regions with a window of 50 sequential homozygous SNPs, allowing for maximum of one mismatch in each homozygous segment. The algorithm CATCH (36) that combines the family pedigree information, ROH and exome sequencing data was used to identify and filter the variants segregating with the disease phenotype in each family. All the segregating filtered variants were analyzed as described in our previous studies (19,59–61) and were confirmed by Sanger capillary sequencing using oligonucleotide primers designed using Primer3 and BLAST (<https://www.ncbi.nlm.nih.gov/tools/primer-blast/>).

Protein modeling

Protein modeling was performed based on the available structure of human FBXL3, which was crystallized in a complex with murine CRY2 and SKP1 proteins. The Protein Data Bank access code is 4I6J (38). The comparison of protein stability between WT and the Cys358Arg mutant was performed using FoldX program (41). Visualization of protein structures and figures were prepared with the University of California, San Francisco (UCSF) Chimera software (62).

Acknowledgements

We thank the Swiss Government Excellence Scholarships program, which provided M.A. the opportunity to work at the University of Geneva Medical School in Switzerland. This project was supported by grants from the ERC 219968 to S.E.A, the Childcare foundation to S.E.A. and the von Meissner Foundation for the grant support to P.M. We also thank all the families for their participation in the study. Molecular graphics and analyses were performed with the UCSF Chimera package developed by

the Resource for Biocomputing, Visualization, and Informatics at the UCSF(supported by NIGMS P41-GM103311).

Conflict of Interest statement. None declared.

References

- Musante, L. and Ropers, H.H. (2014) Genetics of recessive cognitive disorders. *Trends Genet.*, **30**, 32–39.
- Shaffer D.C.M., Bradley S.J., Cantwell .D.P., Carlson, G.A. and Cohen, DMJ (1996) Ross, R. (ed.), *Disorders usually first diagnosed in infancy, childhood, or adolescence* Washington,DC, in press., pp. 37–121.
- Rafiq, M., Ansar, M., Marshall, C., Noor, A., Shaheen, N., Mowjoodi, A., Khan, M., Ali, G., Amin-ud-Din, M. and Feuk, L. (2010) Mapping of three novel loci for non-syndromic autosomal recessive mental retardation (NS-ARMR) in consanguineous families from Pakistan. *Clin. Genet.*, **78**, 478–483.
- Backx, L., Fryns, J.P., Marcelis, C., Devriendt, K., Vermeesch, J. and Van Esch, H. (2010) Haploinsufficiency of the gene Quaking (QKI) is associated with the 6q terminal deletion syndrome. *Am. J. Med. Genet. A*, **152**, 319–326.
- Leonard, H. and Wen, X. (2002) The epidemiology of mental retardation: challenges and opportunities in the new millennium. *Dev. Disabil. Res. Rev.*, **8**, 117–134.
- Maulik, P.K., Mascarenhas, M.N., Mathers, C.D., Dua, T. and Saxena, S. (2011) Prevalence of intellectual disability: a meta-analysis of population-based studies. *Res. Dev. Disabil.*, **32**, 419–436.
- Vissers, L.E., Gilissen, C. and Veltman, J.A. (2016) Genetic studies in intellectual disability and related disorders. *Nat. Rev. Genet.*, **17**, 9–18.
- Willemsen, M. and Kleefstra, T. (2014) Making headway with genetic diagnostics of intellectual disabilities. *Clin. Genet.*, **85**, 101–110.
- Anazi, S., Maddirevula, S., Salpietro, V., Asi, Y.T., Alshahli, S., Alhashem, A., Shamseldin, H.E., AlZahrani, F., Patel, N., Ibrahim, N. et al. (2017) Expanding the genetic heterogeneity of intellectual disability. *Hum. Genet.*, **136**, 1419–1429.
- Anazi, S., Maddirevula, S., Faqeih, E., Alsedairy, H., Alzahrani, F., Shamseldin, H.E., Patel, N., Hashem, M., Ibrahim, N., Abdulwahab, F. et al. (2017) Clinical genomics expands the morbid genome of intellectual disability and offers a high diagnostic yield. *Mol. Psychiatry*, **22**, 615–624.
- Alazami, A.M., Patel, N., Shamseldin, H.E., Anazi, S., Al-Dosari, M.S., Alzahrani, F., Hijazi, H., Alshammari, M., Aldahmesh, M.A., Salih, M.A. et al. (2015) Accelerating novel candidate gene discovery in neurogenetic disorders via whole-exome sequencing of prescreened multiplex consanguineous families. *Cell Rep.*, **10**, 148–161.
- Bittles, A.H. and Black, M. (2010) Evolution in health and medicine Sackler colloquium: consanguinity, human evolution, and complex diseases. *Proc. Natl. Acad. Sci. U. S. A.*, **107**, 1779–1786.
- Kaufman, L., Ayub, M. and Vincent, J.B. (2010) The genetic basis of non-syndromic intellectual disability: a review. *J. Neurodev. Disord.*, **2**, 182.
- Iqbal, Z. and Van Bokhoven, H. (2014) Identifying genes responsible for intellectual disability in consanguineous families. *Hum. Hered.*, **77**, 150–160.
- Jamra, R.A., Wohlfart, S., Zweier, M., Uebe, S., Priebe, L., Ekici, A., Giesebrecht, S., Abboud, A., Al Khateeb, M.A. and Fakher, M. (2011) Homozygosity mapping in 64 Syrian

- consanguineous families with non-specific intellectual disability reveals 11 novel loci and high heterogeneity. *Eur. J. Hum. Genet.*, **19**, 1161–1166.
16. Alkuraya, F. (2013) Impact of new genomic tools on the practice of clinical genetics in consanguineous populations: the Saudi experience. *Clin. Genet.*, **84**, 203–208.
 17. Genomes Project, C., Abecasis, G.R., Auton, A., Brooks, L.D., DePristo, M.A., Durbin, R.M., Handsaker, R.E., Kang, H.M., Marth, G.T. and McVean, G.A. (2012) An integrated map of genetic variation from 1,092 human genomes. *Nature*, **491**, 56–65.
 18. Woods, C.G., Cox, J., Springell, K., Hampshire, D.J., Mohamed, M.D., McKibbin, M., Stern, R., Raymond, F.L., Sandford, R. and Sharif, S.M. (2006) Quantification of homozygosity in consanguineous individuals with autosomal recessive disease. *Am. J. Hum. Genet.*, **78**, 889–896.
 19. Ansar, M., Chung, H.L., Taylor, R.L., Nazir, A., Imtiaz, S., Sarwar, M.T., Manousopoulou, A., Makrythanasis, P., Saeed, S., Falconnet, E. et al. (2018) Bi-allelic loss-of-function variants in DNMBP cause infantile cataracts. *Am. J. Hum. Genet.*, **103**, 568–578.
 20. Najmabadi, H., Hu, H., Garshasbi, M., Zemojtel, T., Abedini, S.S., Chen, W., Hosseini, M., Behjati, F., Haas, S. and Jamali, P. (2011) Deep sequencing reveals 50 novel genes for recessive cognitive disorders. *Nature*, **478**, 57.
 21. Yang, Y., Muzny, D.M., Reid, J.G., Bainbridge, M.N., Willis, A., Ward, P.A., Braxton, A., Beuten, J., Xia, F. and Niu, Z. (2013) Clinical whole-exome sequencing for the diagnosis of mendelian disorders. *N. Engl. J. Med.*, **369**, 1502–1511.
 22. Gilissen, C., Hoischen, A., Brunner, H.G. and Veltman, J.A. (2012) Disease gene identification strategies for exome sequencing. *Eur. J. Hum. Genet.*, **20**, 490–497.
 23. Makrythanasis, P., Nelis, M., Santoni, F.A., Guipponi, M., Vannier, A., Béna, F., Gimelli, S., Stathaki, E., Temtamy, S. and Mégarbané, A. (2014) Diagnostic exome sequencing to elucidate the genetic basis of likely recessive disorders in consanguineous families. *Hum. Mutat.*, **35**, 1203–1210.
 24. Iqbal, Z., Willemsen, M.H., Papon, M.-A., Musante, L., Benevento, M., Hu, H., Venselaar, H., Wissink-Lindhout, W.M., Vulto-van Silfhout, A.T. and Vissers, L.E. (2015) Homozygous SLC6A17 mutations cause autosomal-recessive intellectual disability with progressive tremor, speech impairment, and behavioral problems. *Am. J. Hum. Genet.*, **96**, 386–396.
 25. Makrythanasis, P., Kato, M., Zaki, M.S., Saitou, H., Nakamura, K., Santoni, F.A., Miyatake, S., Nakashima, M., Issa, M.Y. and Guipponi, M. (2016) Pathogenic variants in PIGG cause intellectual disability with seizures and hypotonia. *Am. J. Hum. Genet.*, **98**, 615–626.
 26. Riazuddin, S., Hussain, M., Razaq, A., Iqbal, Z., Shahzad, M., Polla, D., Song, Y., van Beusekom, E., Khan, A. and Tomas-Roca, L. (2016) Exome sequencing of Pakistani consanguineous families identifies 30 novel candidate genes for recessive intellectual disability. *Mol. Psychiatry*, **22**, 1604–1614.
 27. Megarbane, A. and Cormier-Daire, V. (2001) Severe mental retardation, short stature, facial anomalies, joint laxity, and dislocations in two sisters: previously undescribed MCA/MR syndrome. *Am. J. Med. Genet.*, **102**, 153–156.
 28. Wechsler, D. (1997) WAIS-R Scala d'Intelligenza Wechsler per Adulti Riveduta. Giunti O.S, Florence.
 29. Measso, G., Cavarzeran, F., Zappala, G., Lebowitz, B.D., Crook, T.H., Pirozzolo, F.J., Amaducci, L.A., Massari, D. and Grigoletto, F. (1993) The mini-mental-state-examination—normative study of an Italian random sample. *Dev. Neuropsychol.*, **9**, 77–85.
 30. Caffarra, P., Vezzadini, G., Dieci, F., Zonato, F. and Venneri, A. (2002) Rey–Osterrieth complex figure: normative values in an Italian population sample. *Neurol. Sci.*, **22**, 443–447.
 31. Appollonio, I., Leone, M., Isella, V., Piamarta, F., Consoli, T., Villa, M.L., Forapani, E., Russo, A. and Nichelli, P. (2005) The Frontal Assessment Battery (FAB): normative values in an Italian population sample. *Neurol. Sci.*, **26**, 108–116.
 32. Basso, A., Capitani, E. and Laiacona, M. (1987) Raven's coloured progressive matrices: normative values on 305 adult normal controls. *Funct. Neurol.*, **2**, 189–194.
 33. Measso, G., Zappala, G., Cavarzeran, F., Crook, T.H., Romani, L., Pirozzolo, F.J., Grigoletto, F., Amaducci, L.A., Massari, D. and Lebowitz, B.D. (1993) Raven's colored progressive matrices: a normative study of a random sample of healthy adults. *Acta Neurol. Scand.*, **88**, 70–74.
 34. Carlesimo, G.A., Buccione, I., Fadda, L., Graceffa, A., Mauri, M., Lorusso, S., Bevilacqua, G. and Caltagirone, C. (2002) Standardizzazione di due test di memoria per uso clinico: breve racconto e figura di Rey. *Nuova Riv. Neurol.*, **12**, 1–13.
 35. Ferracuti, F. and Ferracuti, S. (1992) Test di Giudizio di Orientamento di Linee. In *Traduzione e Standardizzazione della Versione Italiana*. Giunti O.S, Florence.
 36. Santoni, F.A., Makrythanasis, P. and Antonarakis, S.E. (2015) CATCHing putative causative variants in consanguineous families. *BMC Bioinformatics*, **16**, 310.
 37. Zhang, Z., Duan, Y., Wu, Z., Zhang, H., Ren, J. and Huang, L. (2017) PPAR δ is an inhibitor of cartilage growth in external ears. *Int. J. Biol. Sci.*, **13**, 669–681.
 38. Xing, W., Busino, L., Hinds, T.R., Marionni, S.T., Saifee, N.H., Bush, M.F., Pagano, M. and Zheng, N. (2013) SCF(FBXL3) ubiquitin ligase targets cryptochromes at their cofactor pocket. *Nature*, **496**, 64–68.
 39. Maggi, S., Balzani, E., Lassi, G., Garcia-Garcia, C., Plano, A., Espinoza, S., Mus, L., Tinarelli, F., Nolan, P.M., Gainetdinov, R.R. et al. (2017) The after-hours circadian mutant has reduced phenotypic plasticity in behaviors at multiple timescales and in sleep homeostasis. *Sci. Rep.*, **7**, 17765.
 40. Keers, R., Pedroso, I., Breen, G., Aitchison, K.J., Nolan, P.M., Cichon, S., Nothen, M.M., Rietschel, M., Schalkwyk, L.C. and Fernandes, C. (2012) Reduced anxiety and depression-like behaviours in the circadian period mutant mouse after-hours. *PLoS One*, **7**, e38263.
 41. Guerois, R., Nielsen, J.E. and Serrano, L. (2002) Predicting changes in the stability of proteins and protein complexes: a study of more than 1000 mutations. *J. Mol. Biol.*, **320**, 369–387.
 42. Jin, J., Cardozo, T., Lovering, R.C., Elledge, S.J., Pagano, M. and Harper, J.W. (2004) Systematic analysis and nomenclature of mammalian F-box proteins. *Genes Dev.*, **18**, 2573–2580.
 43. Busino, L., Bassermann, F., Maiolica, A., Lee, C., Nolan, P.M., Godinho, S.I., Draetta, G.F. and Pagano, M. (2007) SCFFbxl3 controls the oscillation of the circadian clock by directing the degradation of cryptochrome proteins. *Science*, **316**, 900–904.
 44. Yoo, S.-H., Mohawk, J.A., Siepkha, S.M., Shan, Y., Huh, S.K., Hong, H.-K., Kornblum, I., Kumar, V., Koike, N. and Xu, M. (2013) Competing E3 ubiquitin ligases govern circadian periodicity by degradation of CRY in nucleus and cytoplasm. *Cell*, **152**, 1091–1105.
 45. Scott, D.C., Rhee, D.Y., Duda, D.M., Kelsall, I.R., Olszewski, J.L., Paulo, J.A., de Jong, A., Ovaa, H., Alpi, A.F. and Harper, J.W. (2016) Two distinct types of E3 ligases work in unison to regulate substrate ubiquitylation. *Cell*, **166**, 1198–1214, e1124.

46. Siepka, S.M., Yoo, S.-H., Park, J., Lee, C. and Takahashi, J.S. (2007) *Cold Spring Harbor Symposia on Quantitative Biology*. Cold Spring Harbor Laboratory Press, Vol. 72, pp. 251–259.
47. Godinho, S.I., Maywood, E.S., Shaw, L., Tucci, V., Barnard, A.R., Busino, L., Pagano, M., Kendall, R., Quwailid, M.M. and Romero, M.R. (2007) The after-hours mutant reveals a role for Fbxl3 in determining mammalian circadian period. *Science*, **316**, 897–900.
48. Busino, L., Bassermann, F., Maiolica, A., Lee, C., Nolan, P.M., Godinho, S.I., Draetta, G.F. and Pagano, M. (2007) SCFFbxl3 controls the oscillation of the circadian clock by directing the degradation of cryptochrome proteins. *Science*, **316**, 900–904.
49. Siepka, S.M., Yoo, S.H., Park, J., Song, W., Kumar, V., Hu, Y., Lee, C. and Takahashi, J.S. (2007) Circadian mutant overtime reveals F-box protein FBXL3 regulation of cryptochrome and period gene expression. *Cell*, **129**, 1011–1023.
50. Hiran, A., Yumimoto, K., Tsunematsu, R., Matsumoto, M., Oyama, M., Kozuka-Hata, H., Nakagawa, T., Lanjakornsiripan, D., Nakayama, K.I. and Fukada, Y. (2013) FBXL21 regulates oscillation of the circadian clock through ubiquitination and stabilization of cryptochromes. *Cell*, **152**, 1106–1118.
51. Maaskant, M., van de Wouw, E., van Wijck, R., Evenhuis, H.M. and Echteld, M.A. (2013) Circadian sleep-wake rhythm of older adults with intellectual disabilities. *Res. Dev. Disabil.*, **34**, 1144–1151.
52. Hare, D.J., Jones, S. and Evershed, K. (2006) Objective investigation of the sleep-wake cycle in adults with intellectual disabilities and autistic spectrum disorders. *J. Intellect. Disabil. Res.*, **50**, 701–710.
53. Mir, A., Sritharan, K., Mittal, K., Vasli, N., Araujo, C., Jamil, T., Rafiq, M.A., Anwar, Z., Mikhailov, A., Rauf, S. et al. (2014) Truncation of the E3 ubiquitin ligase component FBXO31 causes non-syndromic autosomal recessive intellectual disability in a Pakistani family. *Hum. Genet.*, **133**, 975–984.
54. Au, P.Y., Argiropoulos, B., Parboosingh, J.S. and Micheil Innes, A. (2014) Refinement of the critical region of 1q41q42 microdeletion syndrome identifies FBXO28 as a candidate causative gene for intellectual disability and seizures. *Am. J. Med. Genet. A*, **164A**, 441–448.
55. Li, H. and Durbin, R. (2009) Fast and accurate short read alignment with Burrows–Wheeler transform. *Bioinformatics*, **25**, 1754–1760.
56. DePristo, M.A., Banks, E., Poplin, R., Garimella, K.V., Maguire, J.R., Hartl, C., Philippakis, A.A., del Angel, G., Rivas, M.A., Hanna, M. et al. (2011) A framework for variation discovery and genotyping using next-generation DNA sequencing data. *Nat. Genet.*, **43**, 491–498.
57. Pruitt, K.D., Tatusova, T. and Maglott, D.R. (2007) NCBI reference sequences (RefSeq): a curated non-redundant sequence database of genomes, transcripts and proteins. *Nucleic Acids Res.*, **35**, D61–D65.
58. Purcell, S., Neale, B., Todd-Brown, K., Thomas, L., Ferreira, M.A., Bender, D., Maller, J., Sklar, P., de Bakker, P.I., Daly, M.J. et al. (2007) PLINK: a tool set for whole-genome association and population-based linkage analyses. *Am. J. Hum. Genet.*, **81**, 559–575.
59. Makrythanasis, P., Nelis, M., Santoni, F.A., Guipponi, M., Vannier, A., Bena, F., Gimelli, S., Stathaki, E., Temtamy, S., Megarbane, A. et al. (2014) Diagnostic exome sequencing to elucidate the genetic basis of likely recessive disorders in consanguineous families. *Hum. Mutat.*, **35**, 1203–1210.
60. Ansar, M., Riazuddin, S., Sarwar, M.T., Makrythanasis, P., Paracha, S.A., Iqbal, Z., Khan, J., Assir, M.Z., Hussain, M., Razzaq, A. et al. (2018) Biallelic variants in LINGO1 are associated with autosomal recessive intellectual disability, microcephaly, speech and motor delay. *Genet. Med.*, **20**, 778–784.
61. Ansar, M., Chung, H., Waryah, Y.M., Makrythanasis, P., Falconnet, E., Rao, A.R., Guipponi, M., Narsani, A.K., Fingerhut, R., Santoni, F.A. et al. (2018) Visual impairment and progressive phthisis bulbi caused by recessive pathogenic variant in MARK3. *Hum. Mol. Genet.*, **27**, 2703–2711.
62. Pettersen, E.F., Goddard, T.D., Huang, C.C., Couch, G.S., Greenblatt, D.M., Meng, E.C. and Ferrin, T.E. (2004) UCSF Chimera—a visualization system for exploratory research and analysis. *J. Comput. Chem.*, **25**, 1605–1612.